Computational and Structural Biotechnology Journal 20 (2022) 4225–4237

COMPUTATIONAL ANDSTRUCTURAL BIOTECHNOLOGY JOURNAL

journal homepage: www.elsevier.com/locate/csbj

Prediction and validation of host-pathogen interactions by a versatile inference approach using *Aspergillus fumigatus* as a case study

Johannes Balkenhol [a,1], Elena Bencurova [a,1], Shishir K Gupta [b], Hella Schmidt [c], Thorsten Heinekamp [c], Axel Brakhage [c], Aparna Pottikkadavath [d], Thomas Dandekar [a]

[a] Department of Bioinformatics, University of Würzburg, Würzburg, Germany
[b] Evolutionary Genomics Group, Center for Computational and Theoretical Biology, University of Würzburg, 97078 Würzburg, Germany
[c] Department of Molecular and Applied Microbiology, Leibniz Institute for Natural Product Research and Infection Biology (Leibniz-HKI), 07745 Jena, Germany
[d] Department of Structural Biology, Rudolf Virchow Center for Integrative and Translational Bioimaging, University of Würzburg, 97074 Würzburg, Germany

ARTICLE INFO

Article history:
Received 27 March 2022
Received in revised form 29 July 2022
Accepted 29 July 2022
Available online 05 August 2022

Keywords:
Aspergillus fumigatus
host-pathogen interactions
docking
computational prediction
antifungal drugs
ligand binding assay

ABSTRACT

Biological networks are characterized by diverse interactions and dynamics in time and space. Many regulatory modules operate in parallel and are interconnected with each other. Some pathways are functionally known and annotated accordingly, e.g., endocytosis, migration, or cytoskeletal rearrangement. However, many interactions are not so well characterized. For reconstructing the biological complexity in cellular networks, we combine here existing experimentally confirmed and analyzed interactions with a protein-interaction inference framework using as basis experimentally confirmed interactions from other organisms. Prediction scoring includes sequence similarity, evolutionary conservation of interactions, the coexistence of interactions in the same pathway, orthology as well as structure similarity to rank and compare inferred interactions. We exemplify our inference method by studying host-pathogen interactions during infection of *Mus musculus* (phagolysosomes in alveolar macrophages) with *Aspergillus fumigatus* (conidia, airborne, asexual spores). Three of nine predicted critical host-pathogen interactions could even be confirmed by direct experiments. Moreover, we suggest drugs that manipulate the host-pathogen interaction.

1. Introduction

Traditionally, protein-protein interactions (PPI) have been studied on a single-case basis using biochemistry, pharmacological compounds and genetic methods. A considerable number of proteins are encoded by genomes of various organisms. The proteins act rarely alone, but they are connected to dynamic networks that are relevant for cell survival, such as cell architecture, metabolism, and signaling [29]. The reconstruction of protein interaction networks is one of the challenging tasks in modern biology for paving the way to understand the underlying mechanisms of biological processes in time and space [36]. Moreover, the protein interactions are not only crucial for intracellular mechanisms but also for intercellular interactions, such as cell-cell interactions and trans-kingdom communication [46].

However, the traditional methods are neither sufficient nor realistic to detect each PPI. The experimental information on interactions is sparse and only covers a low percentage of all assumed interactions [36]. Therefore, using the knowledge of investigated protein interactions will help to reconstruct an interaction network including intra- and interspecies interactions. Here, we modified the interolog method [56] to infer potential interactions based on already verified interactions. To evaluate predicted interactions, we integrated information from coevolution of proteins, sequence similarity, pathway annotation, as well as micro- and macroscopic relations and the function of the protein network itself [31,36]. Thereby, we constructed a host-pathogen interaction network. As interaction networks do not stop at cell envelopes, host-pathogen interaction networks depend on critical pathogen interactions with the host so that infection can be successful [21,85].

To demonstrate our method, we focused on critical interactions between a mammalian host (*Mus musculus*) and a pathogenic fungus, *Aspergillus fumigatus*.

[1] These authors contributed equally to this work.

E-mail addresses: johannes.balkenhol@uni-wuerzburg.de (J. Balkenhol), elena.bencurova@uni-wuerzburg.de (E. Bencurova), shishir.gupta@uni-wuerzburg.de (S.K Gupta), hella-schmidt@gmx.net (H. Schmidt), thorsten.heinekamp@leibniz-hki.de (T. Heinekamp), axel.brakhage@leibniz-hki.de (A. Brakhage), aparna.pottikkadavath@uni-wuerzburg.de (A. Pottikkadavath), dandekar@biozentrum.uni-wuerzburg.de (T. Dandekar)

https://doi.org/10.1016/j.csbj.2022.07.050

A. fumigatus (*Neosartorya fumigata*) belongs to the saprotrophic fungi decomposing organic material in the soil [3,23]. The fungus mainly reproduces by asexual spores (conidia) which are released into the air. Conidia land on a suitable surface, germinate and after vegetative growth as hyphae, new conidia are formed from conidiophores [39,71]. Various materials including wood, animal nests, and plastic products represent suitable surfaces, however, as a pathogen *A. fumigatus* can survive in the lung of mammals [62]. In humans, *A. fumigatus* can cause life-threatening infections with more than 3,000,000 cases per year [7].

In this study, with a computational approach, we transfer host-pathogen interactions where there are directly measured experimental data to another host organism (e.g. from human to mouse) and another pathogen (e.g. from the fungal pathogen *C. albicans to A. fumigatus*). The interacting domains and their structure have to be conserved in the new organisms, both in the host and the pathogen that such a prediction transfer has success. This is hence a demanding prediction task. To have higher accuracy in our predictions, we combine sequence similarity, evolutionary conservation of interactions, the coexistence of interactions in the same pathway, orthology as well as structure similarity to rank and compare inferred interactions.

Nine of the predicted interactions were tested in a binding assay and we could confirm correct inference and conservation of all required interactions as well as correct working of the interaction assay including protein expression for three such host-pathogen interaction pairs. Moreover, we studied the predicted protein interactions using 3D docking simulations. Finally, we investigated antifungal drugs that potentially manipulate relevant pathogenic proteins for critical protein interactions between the host and the pathogen during the infection.

2. Material and methods

2.1. Protocol of inference

2.1.1. Summary

The interolog prediction is based on verified interactions from seven model species of different kingdoms of life (source network). Derived from the transkingdom network the interspecies interactions of *M. musculus* with *A. fumigatus* were inferred. To evaluate the predicted interactions a scoring system (*predicted_interaction_score*) was introduced. In addition to the *predicted_interaction_score* of interacting proteins, a host-pathogen interaction (HPI) score was calculated. The *hpi_score* integrates information about the properties of the host-pathogen intersection such as virulence or host defense association of certain proteins.

2.1.2. Interaction Data retrieval

The source intraspecies interaction data of *M. musculus*, *A. thaliana*, *S. cerevisiae, D. melanogaster, C. elegans, C. albicans, R. norvegicus, D. rerio,* and *H. sapiens* were downloaded from IntAct [35], BioGRID [49] and further interaction sources of the International Molecular Exchange (IMEx) consortium [48] such as InnateDB [8], MatrixDB [11] and UniProt [73] via PSICQUIC [2] queries. The interactions were filtered according to the interaction type and the interaction detection method (Table S1). The interologs were calculated based on the source networks. The orthologs were determined according to Inparanoid8 [63].

We considered all available interaction data of the most prominent model species (i.e. *M. musculus*, *A. thaliana*, *S. cerevisiae, D. melanogaster, C. elegans, C. albicans, R. norvegicus, D. rerio,* and *H. sapiens*). As we analyzed cross-species interactions of distant species in the phylogenetic tree (human and fungus) it was of particular interest to collect source interactions from species that are also distant in phylogeny. This supports the estimation of conservation of certain interactions, e.g. some relationships of proteins might be very old and some might rather be human or fungi specific. Furthermore, plants and fungi share a long history of close interactions in e.g. mycorrhiza (https://www.nature.com/articles/ncomms1046, accessed 20.07.2022) [94]. Therefore, similar strategies for mutualisms, symbiosis, or pathogenesis might apply for fungus-plant and fungus-human interaction or invasion. In addition, plants can keep a balance in the interaction with fungi, for example with secondary metabolites such as castanospermin, that can silence invasion processes. This metabolite might therefore have a similar silencing effect in fungi-human interaction without directly influencing human signalling. Consequently, plant-fungi interactions might source fungal invasion pathways in humans, and thereby reveal key intersections that can be tackled by compounds of the pool of plant-based metabolites.

2.1.3. Data for predicted interaction scoring based on traits of proteins

Protein traits such as GO association, sequence length, pathway membership, and amino acid sequence similarity were scored to predict and classify protein interactions in the host-pathogen interface.

The Gene Ontology (GO) slim annotations [4] were used to filter genes that are relevant for the HPI (Table S2), as well as to generate a GO correlation network within the interactome considering the GO areas cellular compartment, biological process, and molecular function. The GO slim annotations of *A. fumigatus* proteins and phenotype data (Table S3) of the pathogen were retrieved from the Aspergillus Genome Database [10]. The GO slim data from Ensembl 80 [25] were used to obtain the annotations for the murine host. The local similarity scoring of protein interactions presented in the HPIDB [1] was used to search for similarities of interologs to the host-pathogen interactions. The protein annotation and the protein sequence data were retrieved from Uniprot [74], where the longest sequence was chosen.

The usage of the older Ensembl version is due to the comparison to older datasets of interaction prediction, as well as the time delay between the computation and findings slots for experimental verification. A reanalysis would update certain predicted interactions and might therefore resolve more possible interactions. However, this would not affect the proof of principle of the method that cross-kingdom interactions can be evaluated by hands of intraspecies networks from several model species. In a future version, we strengthen the automation of the prediction pipeline, so that we can regularly follow the updates of all databases used. In these terms, we also intend to combine feature extraction with a learning algorithm. Therefore, a later update of the Ensembl database will be directly accompanied by an update of the prediction method.

2.1.4. Data for the hpi_score based on traits

For ranking the proteins according to their relevance in infection several traits were integrated. The phenotype data (Table S3) indicated infection-relevant proteins by knock-out, knock-down, and overexpression studies were downloaded from the Aspergillus Genome Database [10]. A host-pathogen dual expressions dataset was integrated to evaluate infection-relevant genes in host-fungi interaction as described previously [56]. The proteome data of a phagolysosomes infection model [60] were used to identify proteins that were relevant for the host-pathogen phagolysosomes infection model. The GO terms that indicate the involvement of proteins during the infection were downloaded from the Aspergillus Genome Databank [10] and Ensembl 80 [25]. Protein interactions that are already stated by the HPIDB [1] contribute positively to the *hpi_score*. Further, we searched for proteins that have a transmembrane domain, which indicates surface proteins

thus increasing the chance of being localized at the host-pathogen intersection. The TMHMM data were annotated via the Uniprot database [74].

2.1.5. The scoring

The source interaction score was deduced from the source interaction databases. The Biogrid score was normalized by its median and its quantiles to make it comparable to the IntAct scoring.

For the evaluation of the orthology transfer, the global and local score of the amino acid sequence was calculated. The local score was generated by Blast version 2.2.26, whereas the global score was generated by the Needleman-Wunsch algorithm [44]. The seed ortholog score, determined by the Inparanoid algorithm [63], is set binary. The sequence length score was generated by using the median and quantiles of the sequence length. The pathway score depends on the number of shared pathways [40] and was normalized by the median. Similarly, the GO score depends on the number of shared GO terms and is normalized by the median. For both interaction partners the orthology score is calculated independently (Fig. 1). In consequence, there exist two scores: orthology score1 and orthology score2. The different scorings that contribute to the orthology score are weighted. The weights are manually set. We set the weights intuitive as a starting point for subsequent dynamic weight modulations. However, the setup of weights started from the publication „systematic humanization of yeast" [31] which states a predictability score for various interaction features.

The final *predicted_interaction_score* is a composition of the source interaction score, the *orthology_scores,* and further evaluation of traits of the interacting proteins (Fig. 1). All scores vary between 0 (not interacting) and 1 (interacting). The number of source interactions of each predicted interolog contributed to the overall *predicted_interaction_score*. Additionally, the co-occurrence in the same pathway of the predicted interactions, shared GO terms, coexpression, a high basemean expression, and similarity to known host-pathogen interaction [1] supported the evaluation of the predicted interactions.

orthology_score1/2
= (1 -
(
(1 – percentidentityglobal) *
(1 – percentidentitylocal) *
(1 - 0.2 * bootstrap_as_seed / 100) *
(1 - 0.1 * (seq_length_score)) *
(1 - 0.5 * pathway_score_orth) *
(1 - 0.3 * go_score)
)
)

The overall orthology score is calculated as follows:

orthology_score = orthology_score1 * orthology_score2

The *predicted_interaction_score* uses the source interactions score, the orthology score, and further feature scores that contribute to the characterization of interacting partners.

predicted_interaction_score
= (1 -
(
(1 –
$\prod_{species\ 0}^{species\ n} intactscore * orthology\_score$)*
(1 - 0.1 * (seq_length_score) *
(1 - 0.5 * pathway_score_int) *
(1 - 0.4 * go_score) *
(1 - 0.3 * basemean_score) *
(1 - 0.3 * (hpidb_score))
)
)

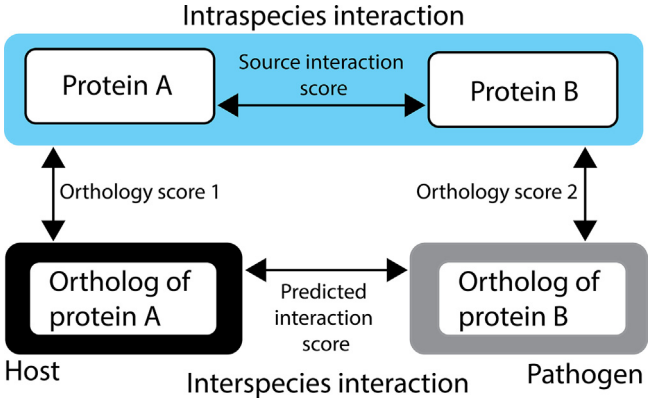

Fig. 1. The prediction of host-pathogen interactions is based on the interolog method using experimentally evaluated interactions partners, named source interaction. The source interaction score is based on the database score of BioGrid and IntAct, which evaluated the experimental method, number of publications describing the interaction and interaction type. To build interologs of the source interaction in a host and pathogen interaction model the orthologs for each interactor were determined. The orthology score is calculated for each interactor and uses the sequence similarity (global and local), co-occurrence in a pathway, GO similarity, sequence length, absolute expression. As a result, the *predicted_interaction_score* of host and pathogen proteins is calculated by the source interactions score, orthology score1 and 2. The *predicted_interaction_score* is further refined by the number of source species predicting the interaction (evolutionary conservation), sequence length, co-occurrence in the same pathway, the GO similarity, the basemean of the expression, as well as the coexpression in an infection model and the similarity to interactions in the HPIDB.

The characterization of proteins in the intersection of host and fungal pathogen allows for evaluating their role in pathogenesis. For this purpose, features that contribute to figuring out the relevance of interactions in pathogenesis are determined. Based on the traits that predict involvement in host-pathogen interactions, such as localization in the outer cell envelope or extracellular space (spatial co-occurrence), coexpression in infection (temporal co-occurrence), the guidance of an infection-related phenotype, a host-pathogen interaction (*hpi_score*) is created. The *hpi_score* gives evidence about the propensity of interaction to occur in the host-pathogen interface and to be relevant for pathogenesis, or to be a potential drug target. The phenotype scores (Table S3) are based on genetic modification studies and were manually curated. The CC_score (GO cellular component) indicates the localization of a protein and was manually curated. Likewise, the BP_score (GO biological process) was determined by infection-relevant BP annotations (Table S2). The phagolysosomes score indicates whether a protein is in the host-pathogen phagolysosomes infection model [60]. Likewise, the degtimepoint score represents the number of times a gene is differentially expressed in a dual RNAseq of host and fungus infection model [56]. The HPIDB score states if the interaction or an interolog is present in the HPIDB. The TMHMM score states whether a protein is located in the membrane of a cell. The phagolysosomes score, the TMHMM score, and the HPIDB score are binary scores and are stated for each protein.

```
hpi_score
= (1 -
    (
      (1 - 0.4 * (0.5 * phenotype_score1 + 0.5 *
  phenotype_score2)) *
      (1 - 0.4 * (phago1 * phago2)) *
      (1 - 0.4 * (0.5 * CC_score1 + 0.5 * CC_score2)) *
      (1 - 0.3 * (0.5 * BP_score1 + 0.5 * BP_score2)) *
      (1 - 0.3 * (0.5 * degtimepoints1 + 0.5 * degtimepoints2))
  *
      (1 - 0.3 * (0.5 * tmhmm1 + 0.5 * tmhmm2)) *
      (1 - 0.3 * (0.5 * hpidb1 + 0.5 * hpidb2))
    )
)
```

The combination of the traits, the weighting, the normalization procedures, and the quality of the score can be evaluated with increasing experimental evidence.

2.2. Mapping the interactions on the phagolysosome infection model

We used the host-pathogen (*M. musculus* – *A. fumigatus*) intersection interactions to model distinct infection models. A proteome dataset from the murine - fungus phagolysosome infection model [60] was retrieved to filter *M. musculus* and *A. fumigatus* proteins that are involved in the infection. For the evaluation of the predicted interactions, we use the scoring framework as shown in Fig. 1. To rank the protein interactions according to their relevance in the infection models we used the *hpi_score*. We filtered the host fungus interaction network for proteins that have a *predicted_interaction_score* > 0.5 and an *hpi_score* > 0.4. The dataset of predicted interaction by the interolog method is large (∼ 100 000 interactions). To narrow down a list of displayable, explorable candidates the dataset was reduced to those interactions with a cutoff *predicted_interaction_score* >0.5 (∼90% quantile, Fig. 2**a**) and *hpi_score* > 0.4 (∼90% quantile) (Fig. 2**b**). This gives a balance of somewhat reliable prediction score and infection-relevant proteins. The median of the predicted interaction score is ∼0.25 and has a maximum. This shows the average performance and prefiltering of the interolog method.

In addition, we filtered the high-scoring protein interaction by the proteome dataset to create a subset of relevant interactions during phagocytosis of *A. fumigatus* (Fig. 3).

2.3. Drug Targets

We screened a compound protein interaction dataset from the STITCH database [70], for interactions that are in the host-pathogen intersection, thus offering a way to manipulate critical interactions between host and pathogen. We filtered compounds that target only *A. fumigatus* proteins and not the murine host. Further, we selected target proteins in *A. fumigatus* that were not orthologous to a murine, or a human protein. The final list of compound protein interaction predictions was sorted according to the *hpi_score*. We manually curated the predicted interactions. The target proteins have a *predicted_interaction_score* > 0.5 and an *hpi_score* > 0.4 in the HPI dataset. However, for the castanospermine targets, AFUA_6G04210 and AFUA_2G12410, the *predicted_interaction_score* and an *hpi_score* were 0.32 and 0.34 (AFUA_6G04210 with LRRK2 (Leucine-rich repeat serine/threonine-protein kinase 2), as well as 0.22 and 0.28 (AFUA_2G12410 with PRKACB (cAMP-dependent protein kinase catalytic subunit beta). Despite castanospermine targets having a *predicted_interaction_score* lower than the threshold it was still considered a good target and was investigated further, as it was predicted to target also *Candida albicans* XOG1 (Eexo-1,3-beta-glucanase).

2.4. Protein preparation

Total RNA isolated from murine phagolysosomes and *A. fumigatus* was reverse transcribed and used to amplify the coding regions of selected proteins (Table 1). The amplification reaction was performed using the DreamTaq Mastermix (Thermo Scientific, Germany). All amplicons were sequenced, digested with restriction enzymes *Bam*HI and *Sal*I (or *Kpn*I, restriction sites are underlined in Table 1), and ligated into pQE-30-UA-mCHERRY-GFP (in-house modified pQE30-UA vector, fused GFP and HIS-tag at C-terminus, Qiagen, Netherlands). Ligation mixtures were purified (Macherey-Nagel, Germany) and used for the transformation of competent cells of *E. coli* strain M15 by heat shock. Transformed cells were plated in LB agar supplemented with 100 μg/ml ampicillin and 25μg/ml kanamycin at 37°C for 12 hours. Expression of recombinant proteins was performed in LB medium with 1mM of IPTG (Merck, Germany) at room temperature for 12 hours. The cell culture was harvested by centrifugation for 10 min at 5,000xg and the pellet was resuspended in ice-cold lysis buffer (50 mM NaH_2PO_4, 300 mM NaCl,10 mM imidazole, 10mM lysozyme) and sonicated. After centrifugation at 12,000x*g* for 30 min at 4°C, soluble proteins were purified using Ni-NTA (Merck, Germany) according to the manufacturer's instruction under denaturing conditions. The presence of proteins was visualized by SDS Page and validated by anti-FLAG (1:10000, Thermo Scientific, Germany) and anti-HIS antibodies (1:1000, Thermo Scientific, Germany).

2.5. Ligand binding assay

Purified fungal proteins (containing only 6xHIS-tag) were separated by SDS-PAGE on 10% (w/v) polyacrylamide gels and electrotransferred onto a nitrocellulose membrane. Membranes were blocked with 5% (w/v) albumin fraction V in 0.05% (w/v) TTBS. After washing, membranes were incubated with 2ml of purified phagolysosomal proteins (tagged with 6xHIS and FLAG-tag). After seven washes with 0.05% (w/v) TTBS, the membrane was incubated with FLAG-HRP conjugated antibody (dilution 1:1000 in 0.5% (w/v) albumin fraction V in 0.05% (w/v) TTBS, Thermo Scientific, Germany) and incubated for 5 min in Super-Signal West Pico ECL substrate (Pierce, Germany). Signals were visualized on a C-digit blot scanner (Licor, Germany).

In our experiments, we expressed three types of proteins: mice proteins were tagged with 6xHIS-tag, FLAG-tag, and GFP (only as expression helper). *Aspergillus* proteins were tagged with 6xHIS and GFP, and finally, GFP protein (control) contained 6xHIS tag. We prepared the following controls: positive control: all proteins were verified with anti-His antibody, we detected signal in each sample. Positive control for mouse/negative control for *Aspergillus* proteins: proteins were detected using anti-FLAG antibody, only mice proteins were detected, and *Aspergillus* proteins were not detectable. The FLAG and 6xHIS tag are both very small peptides, 8 and 6 amino acids, respectively, and their participation in the physical interaction of protein is improbable. For negative control, we used only GFP+6xHIS protein which was allowed to interact with FLAG-tagged proteins, and we did not notice any interaction. A diagram in the supplement shows all controls we used (Suplementary Fig. 1 panel d).

2.6. Structure modeling and docking

We retrieved the amino acid sequences of mouse proteins CDK4, PCNA, and RS14 from the UniProt database [72] and *A. fumigatus* proteins AFUA_1G04950, AFUA_1G15020, AFUA_2G05740,

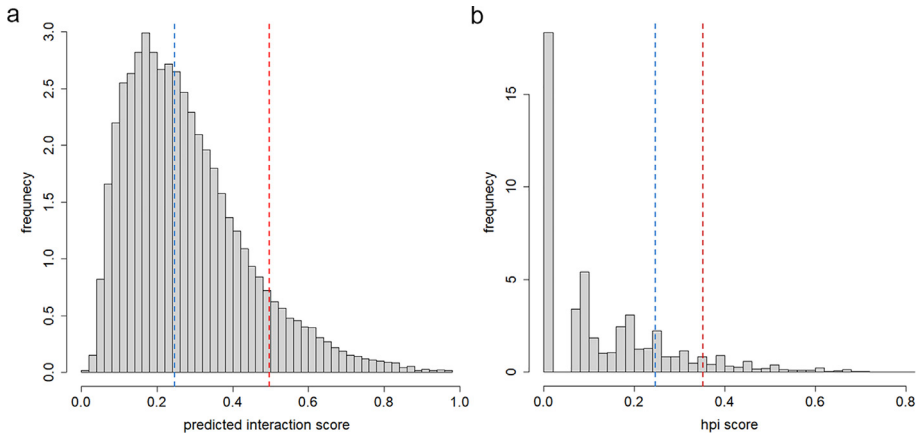

Fig. 2. Histogram of (a) predicted_interesting_score and (b) hpi_score. Breaks = 40. 90% quantile (red line) and median are indicated median (blue line).

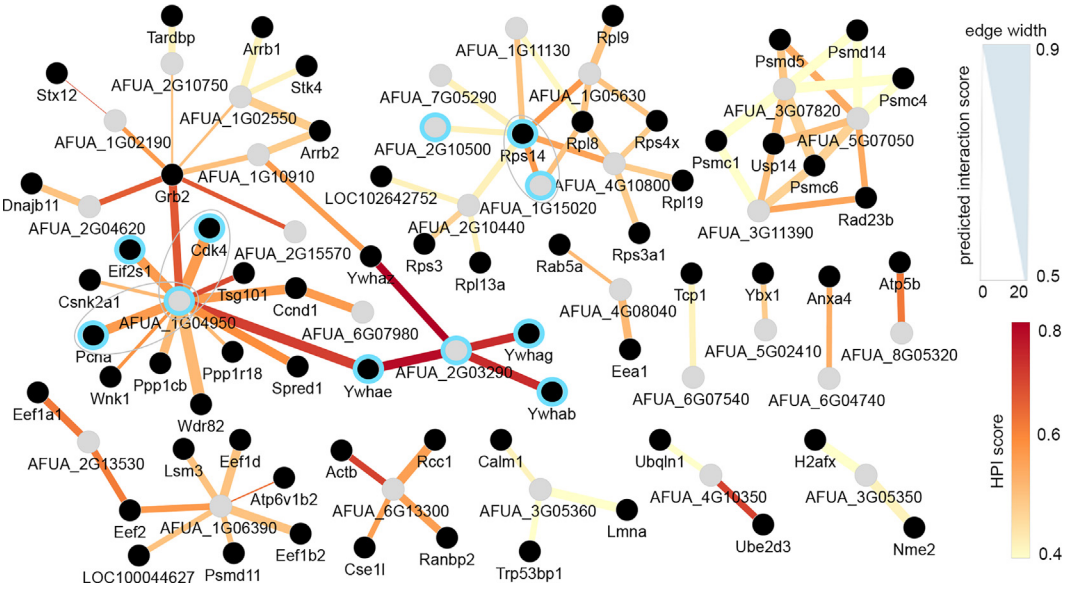

Fig. 3. Protein interactions that are predicted to be relevant in the host-fungus interaction. We show here a subset (*predicted_interaction_score* > 0.4 and *hpi_score* > 0.5) of murine proteins (black node fill) predicted to interact with *A. fumigatus* proteins (grey node fill). The gene names represent the related proteins with the longest sequence. The indicated proteins are identified in the proteome of a phagolysosomes infection model according to Schmidt *et al*. The *predicted_interaction_score* is represented by the edge width and the *hpi_score* is represented by a color code (from 0.4 (yellow) to > 0.8 (red)). Nine of the predicted interactions were investigated in subsequent experiments (blue circles). Three of those interactions could be stated by a Western blot experiment (grey circles with no fill).

AFUA_2G12410, AFUA_5G11970, AFUA_6G04210 and AFUA_7G01220 from the NCBI database (http://www.ncbi.nlm.nih.gov). Three-dimensional (3D) structures of all these proteins were modeled using Phyre2 server [34] which ranks consistently among the top-scoring 3D structure prediction tools in critical assessment of protein structure prediction (CASP) trials [43]. Since energy minimization can repair the deformed geometries by moving atoms to release the internal constraints [64], we subsequently refined all the models using the ModRefiner server [84]. The Psi/Phi Ramachandran plot generated by the PROCHECK [38] program was used to evaluate the quality of the models.

2.6.1. Protein-protein docking

To assess the binding affinity between the pathogen and host proteins we performed protein-protein docking between three pathogen-host pairs AFUA_1G04950 and CDK4, AFUA_1G04950 and PCNA, and AFUA_1G15020 and RS14 using ZDOCK [53]. For each pair, we calculated 1000 poses of interactions and selected the best pose using ZRANK [51]. ZDOCK ranks consistently among the top-scoring tools in Critical Assessment of Predicted Interactions (CAPRI) rounds [28,77]. Moreover, ZRANK-based reranking of docking predictions has shown significant improvement in ZDOCK performance [51–52]. The ZRANK scoring function considers repulsive energies, van der Waals attractive, electrostatic short and long-range attractive, and repulsive energies into calculations [51].

2.6.2. Protein-drug docking

We obtained the structure of 1-benzyl-piperidine hydrochloride (PubChem CID: 13894537), alagebrium chloride (PubChem CID: 13894537), castanospermine (PubChem CID: 13894537), and cuminic acid (PubChem CID: 13894537) from the PubChem database and converted it into 3D structures using Open Babel toolbox [47]. All these ligands and *A. fumigatus* proteins (AFUA_2G05740, AFUA_2G12410, AFUA_5G11970, AFUA_6G04210, and AFUA_7G01220) were prepared for docking using Autodock4 [42]. AutoLigand program [24] was used for the identification of ligand-binding sites in the above-mentioned *A. fumigatus* proteins.

Table 1
Primers used in the study.[1]

Protein *Gene* (Uniprot ID)	Sequence	Organism
40S ribosomal protein S14 *Rps14* (P62264)	F: TTCGGATCCCGCAAGGGGAAGGAAAAG R: TGTGTCGAC*CTTATCGTCGTCATCCTTGTAATC*CACGACGACCCCCTTTTC	*Mus musculus*
Cyclin-dependent kinase 4 *Cdk4* (P30285)	F: CTAGGATCCATGGCTGCCACTCGATATGAA R: TGTGTCGAC*CTTATCGTCGTCATCCTTGTAATC*TGCGTCGCTTTCCTCCTT	*Mus musculus*
Proliferating cell nuclear antigen *Pcna* (P17918)	F: AATGGATCCCTGATCCAGGGCTCCATC R: TGTGTCGAC*CTTATCGTCGTCATCCTTGTAATC*ATCTTCAATCTTGGGAGCCAA	*Mus musculus*
Eukaryotic translation initiation factor 2 subunit 1 *Eif2s1*(Q6ZWX6)	F: CACGGATCCATGCCGGGGCTAAGTTGT R: TGTGTCGAC*CTTATCGTCGTCATCCTTGTAATC*GGCTTCCATTTCTTCTGCATC	*Mus musculus*
14-3-3 protein beta/alpha *Ywhab*(Q9CQV8)	F: ACCGGATCCACCATGGATAAGAGTGAGCTG R: TGTGTCGAC*CTTATCGTCGTCATCCTTGTAATC*GTTCTCTCCCTCTCCAGC	*Mus musculus*
14-3-3 protein epsilon *Ywhae* (P62259)	F: ACCGGATCCGATCGGGAGGATCTGGTG R: TGT*GTCGACCTTATCGTCGTCATCCTTGTAATC*CTGATTCTCATCTTCCACATC	*Mus musculus*
14-3-3 protein gamma *Ywhag*(P61982)	F: ACCGGATCCATGGTGGACCGCGAGCAACTA R: TGTGTCGAC*CTTATCGTCGTCATCCTTGTAATC*GTTGTTGCCTTCACCGCCGTC	*Mus musculus*
14-3-3 family protein ArtA *AFUA_2G03290* (Q4WI29)	F: AACGGATCCATGGGTCACGAAGATGCTGTTTAC R: GTAGTCGACCTCCTCCTTCTTCTCGGCAGG	*Aspergillus fumigatus*
40S ribosomal protein S5 *AFUA_1G15020* (Q4WRU9)	F: GAAGGATCCGATCACGGGGAAGTCGAGGTC R: TATGTCGACAGAGTTGGAGCTTCCCTTGGC	*Aspergillus fumigatus*
Serine/threonine-protein phosphatase *AFUA_1G04950* (Q4WJS6)	F: ATTGGATCCGATAGATTGCTGGAGGTGAGG R: AATGGTACCCTTCTTTGGTTTGCGCGG	*Aspergillus fumigatus*
40S ribosomal protein Rps16 *AFUA_2G10500* (Q4X1C0)	F: TTGGGATCCGTCCCGAGTGTGCAATGCTT R: AATGTCGACGGATTTCTGGTACCTGGCACG	*Aspergillus fumigatus*

[1] Underlined sequences indicate restriction sites. The sequences in *italics* are FLAG-tags. We show only the PCR validation of the protein in the article, however, each gene-coding region was sequenced to validate the proper sequence. Sequences are now added to the supplementary file.

We further performed the docking of 1-benzyl-piperidine hydrochloride into AFUA_7G01220, alagebrium chloride into AFUA_5G11970, castanospermine into AFUA_2G12410 and AFUA_6G04210, and cuminic acid into AFUA_2G05740 in all the predicted ligand-binding sites using Autodock4 implemented in AMDock [75]. The post docking analysis for ligand-protein interactions was performed using Discovery studio visualizer [6].

3. Results

3.1. Computational prediction

3.1.1. Fungus-Host Interface Interactions

Based on experimental evidence for protein interactions we set up an inference method for host-pathogen interactions (Fig. 1). The HPI prediction is based on the interolog method, where the interactions with experimental evidence of several model species were integrated into the host-pathogen network (Fig. 1). The detailed workflow is given in Fig. S3 including a flow chart with description of the data retrieval, integration, prediction method and mapping on an experimental example (proteome analysis phagolysosome).

The orthologs in mice and fungi were determined for each interactor of interactions resulting in a mouse fungus interaction network. To evaluate the predicted interaction each edge of the prediction framework in Fig. 1 was scored (*source_interaction_score*, *orthology_scores*, *predicted_interactions_score*). All scores were integrated to achieve the predicted_interaction_score.

We used different traits to score the predicted interactions (see methods). The HPI network results in 3336 murine proteins, 1281 fungal proteins, and 15446 interactions using a *predicted_interaction_score* > 0.5. The network ranked by the *predicted_interaction_score* is stated in **Table S4**. The filtering of the network for infection-relevant host-pathogen interactions (*hpi_score* > 0.4) resulted in 930 murine proteins, 160 fungal proteins, and 1915 interactions.

Using the inferred networks as a backbone we can model different scenarios, for example, a phagolysosomes infection model and a model for a drug target that manipulates the bottleneck interaction at the intersection site of mouse and fungus.

As an alternative method to the protein interaction predictions, the structural domain comparison can be used [61]. Supplement illustrates how this can be applied to search for possible CD56 protein interactions with fungal proteins (Supplementary material, Table S5). In this case, the structure blast (https://andom.bioapps.biozentrum.uni-wuerzburg.de/index_new.html) examines three-dimensional domains of fungal proteins, which is then compared with the already validated interactions.

3.1.2. Interactions in the phagolysosome infection model

Using our prediction and scoring framework for host-pathogen interactions we created a network to model fungal infection. In Fig. 3 we show the HPI network to model a phagolysosome interaction module of *M. musculus* and *A. fumigatus*. For this, we filtered high-scoring interaction (*predicted_interaction_score* > 0.5 and *hpi_score* > 0.4) and filtered the network by proteome data retrieved from infected murine phagolysosomes [60]. This resulted in an HPI network of 93 infection-relevant interactions with 63 murine proteins and 30 fungal proteins (Fig. 3 and **Table S6**). Fig. 3 shows that different modules have potential infection relevance, such as proteasome modules and modules of extracellular ribosomal proteins. For sorting, we used an interaction method filter and an interaction type filter (as shown in **Table S4**) and calculated a sequence similarity score of the predicted mouse-fungi interactions and the HPIDB interactions.

Furthermore, the serine/threonine protein phosphatase PP1 (AFUA_1G04950) has several high predicted interactions and *hpi_score* interactions with murine proteins, such as: casein kinase 2, alpha 1 polypeptide (Csnk2a1; *predicted_interaction_score*: 0.6;

h*pi_score*: 0.5), the proliferating cell nuclear antigen (Pcna; predicted_interaction_score: 0.6; *hpi_score*: 0.5), the eukaryotic translation initiation factor 2 subunit 1 (Eif2s1; predicted_interaction_score: 0.9; *hpi_score*: 0.6), the cyclin-dependent kinase 4 (Cdk4; predicted_interaction_score: 0.9; *hpi_score*: 0.6), and tyrosine 3-monooxygenase/tryptophan 5-monooxygenase activation proteins (Ywhae; predicted_interaction_score: 0.9; *hpi_score*: 0.7).

The 14-3-3 family protein ArtA (AFUA_2G03290) is predicted to interact with tyrosine 3-monooxygenase/tryptophan 5-monooxygenase activation proteins (Ywhab, Ywhae, Ywhag; respective predicted_interaction_score: 0.8, 0.9, 0.8 and *HPI_score*: ~0.7).

The murine ribosomal protein S14 (Rps14) could interact with the fungal 40S ribosomal protein S5 (AFUA_1G15020; *predicted_interaction_score*: 0.7; *hpi_score*: 0.6) and with fungal 40S ribosomal protein Rps16 (AFUA_2G10500; *predicted_interaction_score*: 0.7; *hpi_score*: 0.5).

Further, it is shown in Fig. 3 that the translation elongation factor EF-1 alpha subunit, putative (AFUA_1G06390) might bind to ATPase, H^+ transporting, lysosomal V_1 subunit B2 (Atp6v1b2). The mitochondrial F1 ATPase subunit alpha (AFUA_8G05320) might bind to ATP synthase, H^+ transporting mitochondrial F1 complex, beta subunit (Atp5b).

The fungal RAB GTPase Ypt5 (AFUA_4G08040) is predicted to interact with the murine early endosome antigen 1 (Eea1; *predicted_interaction_score*: 0.8) and RAB5A, member RAS oncogene family (Rab5a; predicted_interaction_score: 0.6). The interactions have an *hpi_score* of ~0.5.

We tested nine of the interactions experimentally to prove our interaction prediction framework (highlighted in Fig. 3) and to investigate infection-relevant interactions.

3.1.3. Host-Fungus Interface Drug Targets

We searched for drugs that could manipulate protein interactions at the host-pathogen intersection side, as those mark a bottleneck of communication. We searched for drugs that pharmacologically manipulate pathogen proteins and leave the host signaling unaffected.

For this, we deduced bottleneck interactions from the predicted *M. musculus* and *A. fumigatus* HPI network and searched for compounds that interact with the pathogen proteins only. We further filtered for pathogen proteins that have no ortholog on the host species, have a *predicted_interaction_score* > 0.5 and an *hpi_score* > 0.4. The STITCH database [70] states a *combined score* for the compound protein interaction. Here, a *combined score* > 400 was chosen. This yields a medium confidence score, so that no interesting interactions are missed, but the accuracy is still fairly high.

The filtering resulted in the first subset of 120 predicted protein compound interaction at the host-pathogen interface. The table of 120 potential drug-protein interactions was manually curated to find 15 infection-relevant drugs targeting *A. fumigatus* proteins (Table 3).

Most of the drugs exhibited an antifungal/fungicide activity and some of them were supported by literature evidence. The compounds with interesting compound properties and known biological activities were investigated in more detail. One of them is cuminic acid with a benzoic compound group and is known for its antifungal activity towards several plant pathogens, such as *Phytophthora capsica*, *Rhizoctonia cerealis, Gaeumannomyces graminis* var. *tritici*, and *Sclerotinia sclerotiorum* [69]. Cuminic acid is predicted to target the *AFUA_2G05740* gene, a putative Rho-type GTPase that is essential in fungal cell wall construction. The next candidate, 1-benzyl-piperidine hydrochloride is a derivative of another drug, 1-benzylpiperidine. Antifungal activity of derivatives of different benzyl piperidines against *Candida auris* and *Agaricus bisporus* [14,65] makes 1-benzyl piperidine hydrochloride a good candidate as an antifungal compound. AFUA_7G01220 is a potential target of 1- benzyl piperidine hydrochloride. *AFUA_7G01220* encodes for squalene synthase, an enzyme with a role in lanosterol biosynthesis which is part of terpene metabolism. Squalene synthase also plays a role in egosterol synthesis where egosterol was found to be the major membrane sterol in azole-resistant *A. fumigatus* variants [17]. Another drug, castanospermine is known for its highly potent antifungal activity against *S. cerevisiae* and *C. albicans* by inhibiting their exoglucanase activity [12]. For *A. fumigatus,* castanospermine is predicted to target two proteins, AFUA_2G12410 and AFUA_6G04210. AFUA_2G12410 is an uncharacterized protein with predicted domains for mannosyl-oligosaccharide glucosidase activity and the mannosyl-oligosaccharide glucosidase. AFUA_6G04210 encoded protein is involved in processing and remodeling N-glycans in the secretory pathway and is responsible for cell wall synthesis, conidiation germination, and polar growth in *A. fumigatus* [86]. Another candidate, alagebrium chloride contains a phenacyl moiety that has antifungal activity against *C. albicans* and *A. fumigatus* [16]. Alagebrium chloride was predicted to target the protein kinase C AFUA_5G11970, responsible for the cell wall integrity pathway [33]. To check if these compounds have a plausible therapeutic activity against *A. fumigatus*, docking studies were carried out using different compounds with their targeted proteins and it will be discussed later in section 3.2.

3.2. Experimental validation

During the co-evolution, pathogenic fungi have developed several strategies to avoid the harmful host environment, such as different pH, presence of immune cells, or complement-mediated lysis. To resist the destruction caused by the host defense mechanism, recognition and binding to host proteins is one of the mechanisms used by pathogens. To validate the interaction of host proteins with *A. fumigatus*, nine pairs of interacting partners were selected to validate their physical interaction:

1. 40S ribosomal protein S14 (Rps14) and 40S ribosomal protein S5 (AFUA_1G15020)
2. 40S ribosomal protein S14 (Rps14) and 40S ribosomal protein Rps16 (AFUA_2G10500)
3. 14-3-3 protein beta/alpha (Ywhab) and 14-3-3 family protein ArtA (AFUA_2G03290)
4. 14-3-3 protein epsilon (Ywhae) and 14-3-3 family protein ArtA (AFUA_2G03290)
5. 14-3-3 protein epsilon (Ywhae) and serine/threonine-protein phosphatase (AFUA_1G04950)
6. 14-3-3 protein gamma (Ywhag) and 14-3-3 family protein ArtA (AFUA_2G03290)
7. Cyclin-dependent kinase 4 (Cdk4) and serine/threonine-protein phosphatase (AFUA_1G04950)
8. Proliferating cell nuclear antigen (Pcna) and serine/threonine-protein phosphatase (AFUA_1G04950)
9. Eukaryotic translation initiation factor 2 subunit 1 (Eif2s1) and serine/threonine-protein phosphatase (AFUA_1G04950)

Recombinant forms of the selected proteins were produced to validate a single PPI. Correct insertion of the gene of interest into the plasmid was validated by PCR (Table 1, Fig. 4 panel a). After purification, the presence of proteins was validated by SDS-PAGE and using the specific anti-HIS and anti-FLAG antibodies (Fig. 4 panel b, negative controls are depicted in Supplementary Fig. 1). Validation of the interaction was performed by ligand binding assay. The assay showed that three of the predicted nine interaction partners were interacting: 1) 40S ribosomal protein S14 and 40S ribosomal protein S5; 2) proliferating cell nuclear antigen

Table 2
Experimental and computational data confirming host-pathogen interactions

Host	Pathogen	*Predicted_interaction_score*	*Hpi_score*	Derived source interaction	Reference
Cdk4 (Cyclin-dependent kinase 4)	AFUA_1G04950 (Serine/threonine-protein phosphatase)	0.9129	0.5691	CDK4 and PPP1CA/ PPP1CC in human and mouse Cdk4 and Pp1-87B in *D. melanogaster*	[19 67]
Pcna (Proliferating cell nuclear antigen)	AFUA_1G04950 (Serine/threonine-protein phosphatase)	0.8720	0.5691	PCNA and PPP1CC in human and mouse	[19]
Rps14 (40S ribosomal protein S14)	AFUA_1G15020 (Ribosomal protein S5)	0.7265	0.5704	RPS14A and RPS5 in *S. cerevisiae*	[13]

Table 3
Potential manipulations of the host and pathogen communication intersection by drugs. [1]

No	Drug ID (ChEMBL)	Drug	Known activity	Literature evidence	Target genes (*A. fumigatus* homolog)	Description of the target gene (*A. fumigatus* homolog)
1	CHEMBL116158	Cuminic acid	Fungicide	[79,69]	AFUA_2G05740	Putative Rho-type GTPase
2	CHEMBL269311	Pneumocandin B0	Precursor of Caspofungin	—	AFUA_6G12400	Putative 1,3-beta-glucan synthase catalytic subunit, major subunit of glucan synthase
3	CHEMBL437438	L-692289	Like Pneumocandin B0	—	AFUA_6G12400	Putative 1,3-beta-glucan synthase catalytic subunit, major subunit of glucan synthase
4	CHEMBL555311	1-Benzyl-Piperidine Hydrochloride	Antifungal	[14, 87]	AFUA_7G01220	Putative squalene synthetase
5	CHEMBL311226	Castanospermine	Antifungal	[12]	AFUA_2G12410	Has domain(s) with predicted mannosyl-oligosaccharide glucosidase activity
					AFUA_6G04210	Mannosyl-oligosaccharide glucosidase, putative
6	CHEMBL2107309	Alagebrium chloride	Antifungal	[88]	AFUA_5G11970	Protein kinase C, involved in cell wall integrity pathway
7	CHEMBL1236227	N-(4-hydroxybutyl)-phospho-glycolohydroxamic acid	Antifungal	[89]	AFUA_3G11690	Putative class II fructose-bisphosphate aldolase
8	CHEMBL222348	Benzimidazole urea analogue	Antifungal	[90]	AFUA_6G07430	Putative pyruvate kinase
9	CHEMBL272557	Fiacitabine	Anti-HIV and virus	—	AFUA_2G03290	14-3-3 family protein
10	CHEMBL3989494	Siccanin	Antifungal	[91,92]	AFUA_5G11230	Ras family GTPase protein
11	CHEMBL3989665	Alafosfalin	Antifungal	—	AFUA_3G11260	Ubiquitin
12	CHEMBL293961	Benzimidazol derivate	Fungicide	—	AFUA_1G06390	Putative translation elongation factor EF-1 alpha subunit
13	CHEMBL2180480	4-[[5-bromo-4-[(Z)-(2,4-dioxo-3-phenacyl-1,3-thiazolidin-5-ylidene)methyl]-2-ethoxyphenoxy] methyl]benzoic acid	—	[93]	AFUA_6G12400	Putative 1,3-beta-glucan synthase catalytic subunit, major subunit of glucan synthase
14	CHEMBL281926	Bryostatins	—	—	AFUA_5G11970	Protein kinase C, involved in cell wall integrity pathway
15	CHEMBL500316	S)-3-Amino-4-(1H-imidazol-4-yl)-1-phenyl-butan-2-one; dihydrochloride	Like 5-Phenacyl-1H-imidazole	—	AFUA_1G14570	Putative phosphoribosyl-AMP cyclohydrolase

[1] The enlisted drugs were obtained from drug-protein interactions searches in the STITCH database. The targets are proteins in the predicted HPI dataset. The drugs that interact with human or murine proteins were excluded. Targets of the drug are fungal proteins that are not orthologous to human or murine proteins. The STITCH database score was determined to be > 400. The database search for drug-protein relation resulted in 120 interactions. For further refinement of the predicted drug-protein interactions, the table was manually curated, *e.g.*, literature and database search for relevant drugs with implications in infection, resulting in 15 drug-protein interactions.

and Serine/threonine-protein phosphatase; and 3) cyclin-dependent kinase 4 and serine/threonine-protein phosphatase (Fig. 4, panel c). All recombinant proteins were labeled with GFP and His tag, the mouse proteins additionally with FLAG-tag. To avoid non-specific binding, each protein was incubated with GFP-His protein. The negative controls showed no interaction (shown in Supplementary Fig. 1). The source interactions and the predicted interaction score are listed in Table 2.

Among all the evaluated three pathogen-host protein pairs (AFUA_1G04950 and CDK4, AFUA_1G04950 and PCNA, and AFUA_1G15020 and RS14) we identified the top ZRANK score (-109.49) between AFUA_1G04950 and PCNA (Fig. 5**,** panel a). In our recent study, we have identified that PCNA is also a preferential target of the Ebola virus [22]. ZRANK score for AFUA_1G04950-CDK4 (Fig. 5, panel b) and AFUA_1G15020-RS14 (Fig. 5, panel c) was -105.78 and -89.97 respectively. Overall, the docking results complement our experimental findings.

Moreover, we performed docking studies of compounds (see methods) that have shown antifungal activities. The docking studies showed that selected therapeutic agents possess good binding capacities in the binding pocket of receptors with the free energy of binding from -5.63 to -6.79 kcal/mol. Among the tested ligand-receptor pairs castanospermine and uncharacterized protein (AFUA_2G12410), and alagebrium chloride and protein kinase

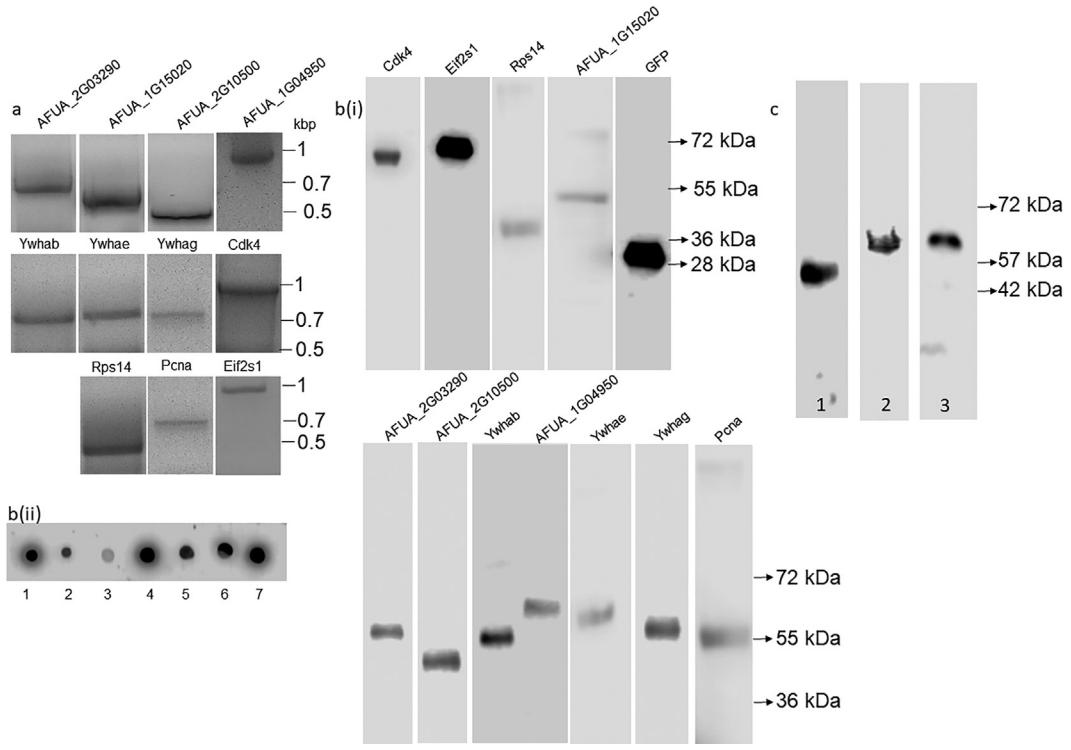

Fig. 4. Experimental validation of selected protein interactions. Panel a – amplicons of seven murine and four *A. fumigatus* genes resolved on the agarose gel. Panel b(i) – purified recombinant proteins detected with anti-HIS antibody. GFP served as a negative control. Panel b(ii) – mice proteins were immobilized on PVDF membrane and hybridized with anti-Flag antibody (input control) [order of proteins: 1 - Ywhab, 2 - Ywhae, 3 - Ywhag, 4 - Cdk4, 5 – Rps14, 6 - Pcna, 7 - Eif2s1. (*A. fumigatus* proteins and GFP were not interacting with anti-FLAG antibody, data in Supplementary Fig. 1)]. Panel C – Interaction between mice and *A. fumigatus* proteins. *A. fumigatus* proteins were immobilized on nitrocellulose membrane and hybridized with purified mice proteins. Interactions were detected with an anti-FLAG antibody. Panel 1 - 40S ribosomal protein S5 (AFUA_1G15020) with 40S ribosomal protein S14(Rps14); panel 2 - Serine/threonine-protein phosphatase (AFUA_1G04950) with Cyclin-dependent kinase 4 (Cdk4); panel 3 - Serine/threonine-protein phosphatase (AFUA_1G04950) with Proliferating cell nuclear antigen (Pcna).

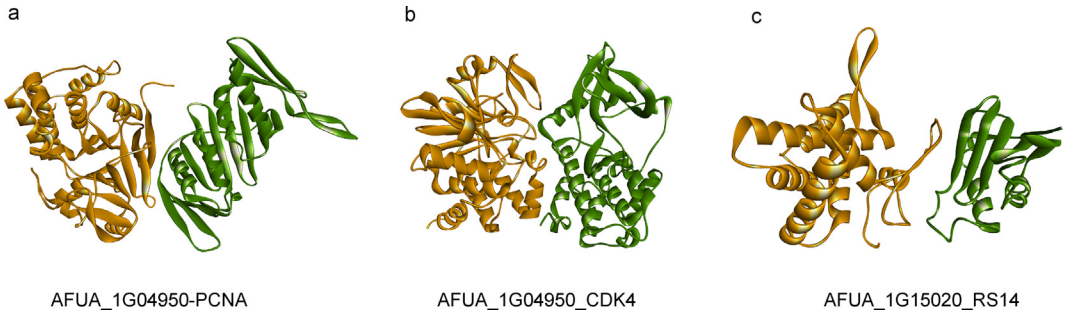

Fig. 5. Protein-protein interaction complex (a) AFUA_1G04950 (orange) and PCNA (green) (b) AFUA_1G04950 (orange) and CDK4 (green) (c) AFUA_1G15020 (orange) and RS14 (green). (For interpretation of the references to colour in this figure legend, the reader is referred to the web version of this article.)

Table 4
Binding affinities between ligand and *A. fumigatus* proteins.

Ligand	Receptor	Free energy of binding (kcal/mol)
Cuminic acid	Cell division control protein 42 homolog AFUA_2G05740	-5.63
1-Benzyl-Piperidine Hydrochloride	Squalene synthase AFUA_7G01220	-5.91
Castanospermine	Uncharacterized protein AFUA_2G12410	-6.79
Castanospermine	Mannosyl-oligosaccharide glucosidase AFUA_6G04210	-6.01
Alagebrium chloride	Protein kinase C AFUA_5G11970	-6.79

C (AFUA_5G11970) showed the highest free energy of binding (Table 4; Fig. S2 panels a-e).

4. Discussion

Infectious diseases remain one of the top five world's deadly diseases. The complex interaction mechanisms between the host and the pathogen are crucial for the invasion, dissemination, and replication of the pathogen in the host. Several bioinformatics strategies have been developed to detect HPI, however, their accuracy is often limited as they were not validated in laboratory experiments. On the other hand, high-throughput experiments such as yeast-two-hybrid or mass spectrometry produce high numbers of false-positive hits, whose filtration is often neither sufficient nor accurate as the single PPI is not possible to validate [41].

We created a method for inferring and scoring (*predicted_interaction_score*) host-pathogen interactions, even between different kingdoms of life. Further, we scored infection-relevant interactions (*hpi_score*) to model pathogenicity-relevant interactions in the inferred network and used a number of further filters and prediction refinements (see methods). A domain interaction database was also in focus, but we decided to exclude the domain interaction from DOMINE database (https://manticore.niehs.nih.gov/cgi-bin/Domine), as we could not state the reliability of the proposed interactions.

The selected interaction protein pairs were subsequently tested in a binding assay to validate our computational prediction method. Here we describe a proof of principle with interesting applications that is already based on a MySQL infrastructure and is therefore easy to transfer via PHP to a web application (see Supplementary Fig. 4). We will improve and automate the pipeline in a subsequent step, as well as add a web interface for easy exploration of the dataset.

It could also be interesting to describe host-pathogen-relevant network modules and intraspecies interactions. However, this was not the focus of our study. We focused here on interspecies interactions as we wanted to deliver a pipeline to identify specifically host-pathogen interactions.

To test the prediction framework, we integrated the host-pathogen interaction with proteomic data of an infection study of *M. musculus* phagolysosomes with *A. fumigatus* conidia [60]. Using the prediction of murine and fungal protein interactions and the temporal and spatial information of the proteins expressed during infection we could identify 93 infection-relevant interactions, of which nine were further analyzed. In the assay, we showed that three of nine selected protein pairs interacted. However, it is necessary to mention that selected proteins were produced in the *E. coli* expression system, which can influence the folding of the proteins, and the assays were performed without the addition of cofactors or other proteins, which may be required for the remaining interactions.

In a 3D protein docking simulation, we collected further insights into the three experimental analyzed interactions.

In addition, we searched for potential drugs that could manipulate the pathogen proteins in the dataset of predicted host-pathogen protein interactions. We identified 16 drugs with potential implications in the host-pathogen interface and analyzed 5 of them in a 3D compound protein docking simulation, where the cuminic acid and 1-benzyl-piperidine hydrochloride showed the highest binding energy to the targeted proteins.

Following the *in silico* analysis, we selected 11 proteins to produce their recombinant forms and to validate their interactions. In a previous study we already used a similar scoring method for refinement of the interolog method [60] . In our current study, we systematically evaluated and refined the scoring, as well as generalized the scoring method to make it applicable for several use cases. We choose here the same use case (phagolysosome) but on a far more challenging comparison (mouse to *A.fumigatus*; many predictions had to be transferred by homology) to build our research on previous investigations (follow-up study, research continuum) and added further evaluation steps to it. We fully outline the scoring method here: We transfer here host-pathogen interactions often from directly measured experimental data to another host organism (e.g. from human to mouse) and often also to another pathogen (e.g. from the fungal pathogen *C.albicans to A.-fumigatus*). The interacting proteins and their structure have to be conserved in the new organisms, both in the host and the pathogen that such a prediction transfer has success. This is hence a demanding prediction task. For best success, we combined different filters such as sequence similarity, evolutionary conservation of interactions as well as the coexistence of interactions in the same pathway, and use both orthology as well as structure similarity to rank and compare inferred interactions. Considering that we need not only correct inference and conservation of all required interactions but also correct working of the interaction assays including the protein expression conditions, the confirmation of three such host-pathogen interaction pairs can be considered a success. Materials and methods explain that the accuracy and success rate can easily be augmented up to nearly fully accurate the closer you get to the direct experimental data and databases which are the basis for our predictions, for instance studying the human host [see also our previous paper; [60]].

The first interaction was detected between the fungal 40S ribosomal protein S5 (AFUA_1G15020, UniProt ID: Q4WRU9) and murine 40S ribosomal protein S14 (Rps14, UniProt ID: P62264). The predicted interaction is derived from the source interaction between RPS14A and RPS5 in *S. cerevisiae* [13]. Both proteins have predicted localization in the extracellular region (GO CC). During the murine phagolysosome infection with *A. fumigatus*, Rps14 is upregulated during infection [60] indicating putative infection relevance. In general, ribosomal proteins have multiple functions including ribosome assembly and maintaining ribosome function, and numerous extraribosomal activities including cell death, transcriptional regulation, and pro-inflammatory signaling during bacterial infection [80]. Interestingly, extracellular functions of ribosomal proteins are currently explored thereby redefining their function [83] and might play a role in immunity [83] and inflammation [18]. In particular, the S5 rRNA is crucial for the formation of ribosomal subunits and interacts with tRNA and other ribosomal proteins, including L5, L18, and L25 [20]. Moreover, it has been identified as an important binding target for translation initiation during virus infections [5]. Also, the Rps14 is involved in numerous interactions mainly with other ribosomal proteins, transcription factors, RNA-binding proteins as well as cytoskeleton-forming and related proteins such as actin and ACTR3B [9,26,27,54]. A recent study found Rps14 to bind to *Salmonella typhimurium* protein SteC, which is required for actin bundling [78]. The interaction between the cytoskeleton and ribosomal proteins is necessary for the cytoskeletal organization and protein connection during the protein synthesis machinery [37], which has been detected also in *A. fumigatus* [30].

Phosphorylation of either host or pathogen proteins is a fundamental event during pathogenesis, allowing adherence, protein-protein interaction, replication, and persistence of the pathogen in host cells [3,32]. Our computational analysis identified serine/threonine-protein phosphatase (SPS (AFUA_1G04950), UniProt ID: Q4WJS6) as the most prominent hub protein with nine interaction partners, from which four were experimentally tested and two were confirmed for the physical interaction *in vitro*; cyclin-dependent kinase 4 (Cdk4, UniProt ID: P30285) and proliferating cell nuclear antigen (Pcna, UniProt ID: P17918) (Fig. 3c). During the infection, SPS is strongly upregulated in wild-type conidia enclosed in murine phagolysosomes which indicates a role in the regulation of replication, translation and transcriptome activity, and cytoskeleton reorganization. Among the host protein, Cdk4 is strongly upregulated, and Pcna is slightly upregulated during infection with *A. fumigatus* [60] showing that both proteins might be relevant for infection. The next step will be to investigate our findings *in vivo* and to characterize the fundamentals of the verified interaction and their importance during infection. In this paper, we only focused on a computational method to analyze and reveal key host-pathogen interactions. In addition, we verified several putative interaction partners as evidence that our method is applicable to research on host-pathogen interactions and can facilitate the search for interacting partners. An *in vivo* evaluation

would provide answers to very important questions, and we hope to continue to unravel these interactions and their role in infection in future.

Predictions on drugs potentially manipulating host and pathogen communication and protein-ligand docking studies revealed promising drug candidates. Castanospermin is a natural alkaloid and its clinical drug alternative celgosivir has proven to have different cancer, as well as antiviral applications [55,58,81,82], and was recently suggested as COVID-19 therapeutic [59]. Additionally, castanospermine is a good inhibitor for different glycosidases in *A. fumigatus*, and exoglucanases in *S. cerevisiae* and *C. albicans* [15,57]. In our study, the prediction of castanospermine targeting mannosyl-oligosaccharide glucosidase with high free energy of binding (-6.01 kcal/mol) suggests castanospermine as a potential target against *A. fumigatus*. Alagebrium chloride is an advanced glycation endproduct breaker that reverses one of the ageing mechanisms [76]. Its N-phenacyl imidazole moiety is known for its antifungal activity [45,66]. The prediction to target protein kinase C with a high free binding energy of 6.70 kcal/mol, alagebrium chloride ranges as a potential drug against *A. fumigatus*. Cuminic acid is a well-known fungicide for plants and it is proven to be environmentally friendly [50]. Different studies showed it harms no plants in some cases cuminic acid enhances the plant's defense mechanism [68,79]. Targeting genes that are responsible for cell wall integrity and polarity with a predicted high free binding energy (-5.63 kcal/mol) cuminic acid also stands out as a potential drug against *A. fumigatus*. 1-Benzyl-piperidine hydrochloride targeting gene encodes squalene synthase involved in ergosterol synthesis pathway. This could indicate 1-Benzyl-piperidine hydrochloride is organism friendly as it targets a unique fungi sterol. With a -5.91 kcal/mol free binding energy, 1-Benzyl-piperidine hydrochloride can be speculated as a potential drug candidate against *A.fumigatus*. Based on our analysis, we suggest here two clinically approved drugs and two compounds not yet approved to be investigated for benefits in *A.fumigatus* infection.

5. Conclusion

We developed a framework for predicting transkingdom interactions and investigated several host-pathogen interactions *in silico* and also *in vitro*. Our data prove that the prediction framework helps to narrow down potential infection-relevant interaction candidates that could be validated in subsequent experiments. Moreover, three protein pairs are experimentally validated and involved in the host-pathogen interaction.

The identified drug-protein interactions can be used as leads for new therapeutic strategies in fungal infections.

Further experimental validation is necessary to claim the effectiveness of our findings for future antifungal treatment.

Data availability statement

All data are available from the manuscript and its supplemental materials.

CRediT authorship contribution statement

Johannes Balkenhol: Conceptualization. **Elena Bencurova:** Conceptualization, Investigation, Methodology, Validation, Writing - original draft, Writing - review & editing. **Shishir K. Gupta:** authorship contribution statement: Investigation, Methodology, formal analysis. **Hella Schmidt:** Conceptualization, Investigation, Writing - review & editing. **Thorsten Heinekamp:** Conceptualization, Supervision. **Axel Brakhage:** Supervision, Funding acquisition, Project administration. **Aparna Pottikkadavath:** authorship contribution statement: Investigation, Methodology, formal analysis. **Thomas Dandekar:** Conceptualization, Supervision, Formal analysis, Funding acquisition, Investigation, Project administration, Writing - original draft, Writing - review & editing.

Declaration of Competing Interest

The authors declare that they have no known competing financial interests or personal relationships that could have appeared to influence the work reported in this paper.

Acknowledgements

We thank the Deutsche Forschungsgemeinschaft (DFG) Collaborative Research Center/Transregio 124 FungiNet for funding (project number 210879364/TR124-B1; J.B. acknowledges funding by 210879364/TR124-B2; H.S. and A.A.B acknowledge funding by 210879364/TR124-A1).

Appendix A. Supplementary data

Supplementary data to this article can be found online at https://doi.org/10.1016/j.csbj.2022.07.050.

References

[1] Ammari, M.G., Gresham, C.R., McCarthy, F.M., and Nanduri, B. (2016). HPIDB 2.0: a curated database for host-pathogen interactions. Database (Oxford) *2016*.
[2] Aranda B, Blankenburg H, Kerrien S, Brinkman FS, Ceol A, Chautard E, et al. PSICQUIC and PSISCORE: accessing and scoring molecular interactions. Nat Methods 2011;8:528–9.
[3] Arastehfar A, Carvalho A, Houbraken J, Lombardi L, Garcia-Rubio R, Jenks JD, et al. *Aspergillus fumigatus* and aspergillosis: from basics to clinics. Stud Mycol 2021;100:100115.
[4] Ashburner M, Ball CA, Blake JA, Botstein D, Butler H, Cherry JM, et al. Gene ontology: tool for the unification of biology. The Gene Ontology Consortium. Nat Genet 2000;25:25–9.
[5] Bhat P, Shwetha S, Sharma DK, Joseph AP, Srinivasan N, Das S. The beta hairpin structure within ribosomal protein S5 mediates interplay between domains II and IV and regulates HCV IRES function. Nucleic Acids Res 2015;43:2888–901.
[6] Biovia DS. Discovery studio visualizer. San Diego, CA, USA; 2017 *936*.
[7] Bongomin F, Gago S, Oladele RO, Denning DW. Global and multi-national prevalence of fungal diseases-estimate precision. J Fungi (Basel) 2017:3.
[8] Breuer K, Foroushani AK, Laird MR, Chen C, Sribnaia A, Lo R, et al. InnateDB: systems biology of innate immunity and beyond–recent updates and continuing curation. Nucleic Acids Res 2013;41:D1228–33.
[9] Capalbo L, Bassi ZI, Geymonat M, Todesca S, Copoiu L, Enright AJ, et al. The midbody interactome reveals unexpected roles for PP1 phosphatases in cytokinesis. Nat Commun 2019;10.
[10] Cerqueira GC, Arnaud MB, Inglis DO, Skrzypek MS, Binkley G, Simison M, et al. The Aspergillus Genome Database: multispecies curation and incorporation of RNA-Seq data to improve structural gene annotations. Nucleic Acids Res 2014;42:D705–10.
[11] Chautard E, Fatoux-Ardore M, Ballut L, Thierry-Mieg N, Ricard-Blum S. MatrixDB, the extracellular matrix interaction database. Nucleic Acids Res 2011;39:D235–40.
[12] Childers DS, Avelar GM, Bain JM, Pradhan A, Larcombe DE, Netea MG, Erwig LP, Gow NAR, Brown AJP. Epitope Shaving Promotes Fungal Immune Evasion. mBio; 2011, *11*.
[13] Collins SR, Kemmeren P, Zhao XC, Greenblatt JF, Spencer F, Holstege FC, et al. Toward a comprehensive atlas of the physical interactome of *Saccharomyces cerevisiae*. Mol Cell Proteomics 2007;6:439–50.
[14] De Luca L, Germano MP, Fais A, Pintus F, Buemi MR, Vittorio S, et al. Discovery of a new potent inhibitor of mushroom tyrosinase (*Agaricus bisporus*) containing 4-(4-hydroxyphenyl)piperazin-1-yl moiety. Bioorg Med Chem 2020;28:115497.
[15] Elbein AD, Mitchell M, Molyneux RJ. Effect of castanospermine on the structure and secretion of glycoprotein enzymes in *Aspergillus fumigatus*. J Bacteriol 1984;160:67–75.
[16] Emami S, Foroumadi A, Falahati M, Lotfali E, Rajabalian S, Ebrahimi SA, et al. 2-Hydroxyphenacyl azoles and related azolium derivatives as antifungal agents. Bioorg Med Chem Lett 2008;18:141–6.
[17] Ferreira ME, Colombo AL, Paulsen I, Ren Q, Wortman J, Huang J, et al. The ergosterol biosynthesis pathway, transporter genes, and azole resistance in *Aspergillus fumigatus*. Med Mycol 2005;43(Suppl 1):S313–9.

[18] Filip AM, Klug J, Cayli S, Frohlich S, Henke T, Lacher P, et al. Ribosomal protein S19 interacts with macrophage migration inhibitory factor and attenuates its pro-inflammatory function. J Biol Chem 2009;284:7977–85.
[19] Flores-Delgado G, Liu CWY, Sposto R, Berndt N. A limited screen for protein interactions reveals new roles for protein phosphatase 1 in cell cycle control and apoptosis. J Proteome Res 2007;6:1165–75.
[20] Gongadze GM. 5S rRNA and ribosome. Biochemistry (Mosc) 2011;76:1450–64.
[21] Greer R, Dong X, Morgun A, Shulzhenko N. Investigating a holobiont: Microbiota perturbations and transkingdom networks. Gut Microbes 2016;7:126–35.
[22] Gupta SK, Ponte-Sucre A, Bencurova E, Dandekar T. An Ebola, Neisseria and Trypanosoma human protein interaction census reveals a conserved human protein cluster targeted by various human pathogens. Comput Struct Biotechnol J 2021;19:5292–308.
[23] Gupta SK, Srivastava M, Osmanoglu O, Xu Z, Brakhage AA, Dandekar T. *Aspergillus fumigatus* versus Genus Aspergillus: Conservation, Adaptive Evolution and Specific Virulence Genes. Microorganisms; 2021b 9.
[24] Harris R, Olson AJ, Goodsell DS. Automated prediction of ligand-binding sites in proteins. Proteins 2008;70:1506–17.
[25] Howe KL, Achuthan P, Allen J, Allen J, Alvarez-Jarreta J, Amode MR, et al. Ensembl 2021. Nucleic Acids Res 2021;49:D884–91.
[26] Huttlin EL, Bruckner RJ, Paulo JA, Cannon JR, Ting L, Baltier K, et al. Architecture of the human interactome defines protein communities and disease networks. Nature 2017;545:505-+.
[27] Huttlin EL, Ting L, Bruckner RJ, Gebreab F, Gygi MP, Szpyt J, et al. The BioPlex Network: A Systematic Exploration of the Human Interactome. Cell 2015;162:425–40.
[28] Hwang H, Vreven T, Pierce BG, Hung JH, Weng Z. Performance of ZDOCK and ZRANK in CAPRI rounds 13–19. Proteins 2010;78:3104–10.
[29] Jones S, Thornton JM. Principles of protein-protein interactions. Proc Natl Acad Sci U S A 1996;93:13–20.
[30] Juvvadi PR, Belina D, Soderblom EJ, Moseley MA, Steinbach WJ. Filamentous fungal-specific septin AspE is phosphorylated in vivo and interacts with actin, tubulin and other septins in the human pathogen *Aspergillus fumigatus*. Biochem Bioph Res Co 2013;431:547–53.
[31] Kachroo AH, Laurent JM, Yellman CM, Meyer AG, Wilke CO, Marcotte EM. Evolution. Systematic humanization of yeast genes reveals conserved functions and genetic modularity. Science 2015;348:921–5.
[32] Kaltdorf M, Srivastava M, Gupta SK, Liang C, Binder J, Dietl AM, et al. Systematic identification of anti-fungal drug targets by a metabolic network approach. Front Mol Biosci 2016;3:22.
[33] Katayama T, Uchida H, Ohta A, Horiuchi H. Involvement of protein kinase C in the suppression of apoptosis and in polarity establishment in *Aspergillus nidulans* under conditions of heat stress. PLoS ONE 2012;7:e50503.
[34] Kelley LA, Mezulis S, Yates CM, Wass MN, Sternberg MJ. The Phyre2 web portal for protein modeling, prediction and analysis. Nat Protoc 2015;10:845–58.
[35] Kerrien S, Aranda B, Breuza L, Bridge A, Broackes-Carter F, Chen C, et al. The IntAct molecular interaction database in 2012. Nucleic Acids Res 2012;40:D841–6.
[36] Keskin O, Tuncbag N, Gursoy A. Predicting protein-protein interactions from the molecular to the proteome level. Chem Rev 2016;116:4884–909.
[37] Kusui K, Sasaki H, Adachi R, Matsui S, Yamamoto K, Yamaguchi T, et al. Ribosomal protein S18 identified as a cofilin-binding protein by using phage display library. Mol Cell Biochem 2004;262:187–93.
[38] Laskowski RA, Macarthur MW, Moss DS, Thornton JM. Procheck – a program to check the stereochemical quality of protein structures. J Appl Crystallogr 1993;26:283–91.
[39] Latge JP, Chamilos G. *Aspergillus fumigatus* and aspergillosis in 2019. Clin Microbiol Rev 2019;33.
[40] Mi H, Thomas P. PANTHER pathway: an ontology-based pathway database coupled with data analysis tools. Methods Mol Biol 2009;563:123–40.
[41] Montanez G, Cho YR. Predicting false positives of protein-protein interaction data by semantic similarity measures. Curr Bioinform 2013;8:339–46.
[42] Morris GM, Huey R, Olson AJ. Using AutoDock for ligand-receptor docking. Curr Protoc Bioinformatics *Chapter 8*, Unit 8 14; 2008.
[43] Moult J, Fidelis K, Kryshtafovych A, Schwede T, Tramontano A. Critical assessment of methods of protein structure prediction (CASP)–round x. Proteins 2014;82(Suppl 2):1–6.
[44] Needleman SB, Wunsch CD. A general method applicable to the search for similarities in the amino acid sequence of two proteins. J Mol Biol 1970;48:443–53.
[45] Nelson R, Kesternich V, Pérez-Fehrmann M, Salazar F, Marcourt L, Christen P, et al. Synthesis and antifungal activity of phenacyl azoles. J Chem Res 2014;38:549–52.
[46] Nishimoto A, Wohlgemuth N, Rosch J, Schultz-Cherry S, Cortez V, Rowe HM. Transkingdom interactions important for the pathogenesis of human viruses. J Infect Dis 2021;223:S201–8.
[47] O'Boyle NM, Banck M, James CA, Morley C, Vandermeersch T, Hutchison GR. Open Babel: An open chemical toolbox. J Cheminform 2011;3:33.
[48] Orchard S, Kerrien S, Abbani S, Aranda B, Bhate J, Bidwell S, et al. Protein interaction data curation: the International Molecular Exchange (IMEx) consortium. Nat Methods 2012;9:345–50.
[49] Oughtred R, Rust J, Chang C, Breitkreutz BJ, Stark C, Willems A, et al. The BioGRID database: A comprehensive biomedical resource of curated protein, genetic, and chemical interactions. Protein Sci 2021;30:187–200.
[50] Park JH, Choi GJ, Jang KS, Lim HK, Kim HT, Cho KY, et al. Antifungal activity against plant pathogenic fungi of chaetoviridins isolated from *Chaetomium globosum*. FEMS Microbiol Lett 2005;252:309–13.
[51] Pierce B, Weng Z. ZRANK: reranking protein docking predictions with an optimized energy function. Proteins 2007;67:1078–86.
[52] Pierce B, Weng Z. A combination of rescoring and refinement significantly improves protein docking performance. Proteins 2008;72:270–9.
[53] Pierce BG, Wiehe K, Hwang H, Kim BH, Vreven T, Weng Z. ZDOCK server: interactive docking prediction of protein-protein complexes and symmetric multimers. Bioinformatics 2014;30:1771–3.
[54] Pourhaghighi R, Ash PEA, Phanse S, Goebels F, Hu LZM, Chen S, et al. BraInMap elucidates the macromolecular connectivity landscape of mammalian brain (vol 10, pg 333, 2020). Cell Syst 2020;11:208.
[55] Rathore AP, Paradkar PN, Watanabe S, Tan KH, Sung C, Connolly JE, et al. Celgosivir treatment misfolds dengue virus NS1 protein, induces cellular pro-survival genes and protects against lethal challenge mouse model. Antiviral Res 2011;92:453–60.
[56] Remmele CW, Luther CH, Balkenhol J, Dandekar T, Muller T, Dittrich MT. Integrated inference and evaluation of host-fungi interaction networks. Front Microbiol 2015;6:764.
[57] Ridruejo JC, Munoz MD, Andaluz E, Larriba G. Inhibition of yeast exoglucanases by glucosidase inhibitors. Biochim Biophys Acta 1989;993:179–85.
[58] Ruprecht RM, Bernard LD, Bronson R, Gama Sosa MA, Mullaney S. Castanospermine vs. its 6-O-butanoyl analog: a comparison of toxicity and antiviral activity in vitro and in vivo. J Acquir Immune Defic Syndr (1988) 4, 48-55.
[59] Santos-Beneit F, Raskevicius V, Skeberdis VA, Bordel S. A metabolic modeling approach reveals promising therapeutic targets and antiviral drugs to combat COVID-19. Sci Rep 2021;11:11982.
[60] Schmidt H, Vlaic S, Kruger T, Schmidt F, Balkenhol J, Dandekar T, et al. Proteomics of *Aspergillus fumigatus* conidia-containing phagolysosomes identifies processes governing immune evasion. Mol Cell Proteomics 2018;17:1084–96.
[61] Schmidt S, Bork P, Dandekar T. A versatile structural domain analysis server using profile weight matrices. J Chem Inf Comp Sci 2002;42:405–7.
[62] Seyedmousavi S, Guillot J, Arne P, de Hoog GS, Mouton JW, Melchers WJ, et al. *Aspergillus* and aspergilloses in wild and domestic animals: a global health concern with parallels to human disease. Med Mycol 2015;53:765–97.
[63] Sonnhammer EL, Ostlund G. InParanoid 8: orthology analysis between 273 proteomes, mostly eukaryotic. Nucleic Acids Res 2015;43:D234–9.
[64] Srivastava M, Gupta SK, Abhilash PC, Singh N. Structure prediction and binding sites analysis of curcin protein of Jatropha curcas using computational approaches. J Mol Model 2012;18:2971–9.
[65] Srivastava V, Wani MY, Al-Bogami AS, Ahmad A. Piperidine based 1,2,3-triazolylacetamide derivatives induce cell cycle arrest and apoptotic cell death in *Candida auris*. J Adv Res 2021;29:121–35.
[66] Staniszewska M, Kuryk L, Gryciuk A, Kawalec J, Rogalska M, Baran J, Kowalkowska A. The Antifungal Action Mode of N-Phenacyldibromobenzimidazoles. Molecules; 2021, *26*.
[67] Stanyon CA, Liu GZ, Mangiola BA, Patel N, Giot L, Kuang B, et al. A Drosophila protein-interaction map centered on cell-cycle regulators. Genome Biol 2004:5.
[68] Sun Y, Wang Y, Han LR, Zhang X, Feng JTx. Antifungal Activity and Action Mode of Cuminic Acid from the Seeds of Cuminum cyminum L. against *Fusarium oxysporum f. sp. Niveum* (FON) Causing Fusarium Wilt on Watermelon. Molecules; 2017, *22*.
[69] Sun Y, Wang Y, Xie ZY, Guo EH, Han LR, Zhang X, et al. Activity and biochemical characteristics of plant extract cuminic acid against *Sclerotinia sclerotiorum*. Crop Prot 2017;101:76–83.
[70] Szklarczyk D, Santos A, von Mering C, Jensen LJ, Bork P, Kuhn M. STITCH 5: augmenting protein-chemical interaction networks with tissue and affinity data. Nucleic Acids Res 2016;44:D380–4.
[71] Teertstra WR, Tegelaar M, Dijksterhuis J, Golovina EA, Ohm RA, Wosten HAB. Maturation of conidia on conidiophores of *Aspergillus niger*. Fungal Genet Biol 2017;98:61–70.
[72] The UniProt C. UniProt: the universal protein knowledgebase. Nucleic Acids Res 2017;45:D158–69.
[73] UniProt C. UniProt: a hub for protein information. Nucleic Acids Res 2015;43:D204–12.
[74] UniProt C. UniProt: the universal protein knowledgebase in 2021. Nucleic Acids Res 2021;49:D480–9.
[75] Valdes-Tresanco MS, Valdes-Tresanco ME, Valiente PA, Moreno E. AMDock: a versatile graphical tool for assisting molecular docking with Autodock Vina and Autodock4. Biol Direct 2020;15:12.
[76] Vasan S, Zhang X, Zhang X, Kapurniotu A, Bernhagen J, Teichberg S, et al. An agent cleaving glucose-derived protein crosslinks in vitro and in vivo. Nature 1996;382:275–8.
[77] Vreven T, Vangaveti S, Borrman TM, Gaines JC, Weng Z. Performance of ZDOCK and IRAD in CAPRI rounds 39–45. Proteins 2020;88:1050–4.
[78] Walch P, Selkrig J, Knodler LA, Rettel M, Stein F, Fernandez K, et al. Global mapping of Salmonella enterica-host protein-protein interactions during infection. Cell Host Microbe 2021;29:1316-+.
[79] Wang Y, Zhang J, Sun Y, Feng J, Zhang X. Evaluating the potential value of natural product cuminic acid against plant pathogenic fungi in cucumber. Molecules 2017;22.

[80] Warner JR, McIntosh KB. How common are extraribosomal functions of ribosomal proteins? Mol Cell 2009;34:3–11.
[81] Whitby K, Taylor D, Patel D, Ahmed P, Tyms AS. Action of celgosivir (6 O-butanoyl castanospermine) against the pestivirus BVDV: implications for the treatment of hepatitis C. Antivir Chem Chemother 2004;15:141–51.
[82] Wojtowicz K, Januchowski R, Sosinska P, Nowicki M, Zabel M. Effect of brefeldin A and castanospermine on resistant cell lines as supplements in anticancer therapy. Oncol Rep 2016;35:2896–906.
[83] Xiong W, Lan T, Mo B. Extraribosomal functions of cytosolic ribosomal proteins in plants. Front Plant Sci 2021;12:607157.
[84] Xu D, Zhang Y. Improving the physical realism and structural accuracy of protein models by a two-step atomic-level energy minimization. Biophys J 2011;101:2525–34.
[85] Yu H, Kim PM, Sprecher E, Trifonov V, Gerstein M. The importance of bottlenecks in protein networks: correlation with gene essentiality and expression dynamics. PLoS Comput Biol 2007;3:e59.
[86] Zhang L, Zhou H, Ouyang H, Li Y, Jin C. Afcwh41 is required for cell wall synthesis, conidiation, and polarity in Aspergillus fumigatus. FEMS Microbiol Lett 2008;289:155–65.
[87] Srivastava V, Wani MY, Al-Bogami AS, Ahmad A. Piperidine based 1,2,3-triazolylacetamide derivatives induce cell cycle arrest and apoptotic cell death in Candida auris. J Adv Res 2021;29:121–35. https://doi.org/10.1016/j.jare.2020.11.002.
[88] Cooper ME, Thallas V, Forbes J, Scalbert E, Sastra S, Darby I, et al. The cross-link breaker, N-phenacylthiazolium bromide prevents vascular advanced glycation end-product accumulation. Diabetologia 2000;43(5):660–4.
[89] Daher R, Coinçon M, Fonvielle M, Gest PM, Guerin ME, Jackson M, et al. Rational design, synthesis, and evaluation of new selective inhibitors of microbial class II (zinc dependent) fructose bis-phosphate aldolases. Journal of medicinal chemistry 2010;53(21):7836–42.
[90] Mani N, Gross CH, Parsons JD, Hanzelka B, Muħ U, Mullin S, et al. In vitro characterization of the antibacterial spectrum of novel bacterial type II topoisomerase inhibitors of the aminobenzimidazole class. Antimicrobial Agents and Chemotherapy 2006;50(4):1228–37.
[91] Bellotti MG, Riviera L. Siccanin: a new antifungal antibiotic with antidermatophytic properties. In vitro studies. Chemioterapia: International Journal of the Mediterranean Society of Chemotherapy 1985;4(6):431–3.
[92] Sugawara S. Siccanin, a new antifungal antibiotic. II. In vivo studies. Siccanin, a new antifungal antibiotic. In vivo studies. 1970:253–6.
[93] Li P, Tan JJ, Liu M, Zhang XY, Chen WZ, Wang CX. Insight into the inhibitory mechanism and binding mode between D77 and HIV-1 integrase by molecular modeling methods. Journal of Biomolecular Structure and Dynamics 2011;29(2):311–23.
[94] Bonfante P, Genre A. Mechanisms underlying beneficial plant–fungus interactions in mycorrhizal symbiosis. Nat Commun 2010;1:48.